GEO DEBRIS AND INTERPLANETARY DUST: FLUXES AND CHARGING BEHAVIOR

A. L. Graps[1]**, Green, S.F.**[2]**, McBride, N.**[2]**, McDonnell, J.A.M.**[3]**, Bunte, K.**[4]**, Svedhem, H.**[5]**, and Drolshagen, G.**[5]

[1]*INAF Istituto di Fisica dello Spazio Interplanetario, CNR-ARTOV, Via del Fosso del Cavaliere 100, 00133 Rome, Italy,*
Amara.Graps@ifsi-roma.inaf.it
[2]*PSSRI, The Open University, Walton Hall, Milton Keynes MK7 6AA, U.K.*
[3]*Unispace Kent, P.O. Box 318, Canterbury, Kent CT2 8HB, U.K.*
[4]*eta_max space GmbH, Richard-Wagner-Strasse 1, D-38106 Braunschweig, Germany*
[5]*ESA/ESTEC, PB 299, NL-2200 AG Noordwijk, The Netherlands*

ABSTRACT

In September 1996, a dust/debris detector: GORID was launched into the geostationary (GEO) region as a piggyback instrument on the Russian Express-2 telecommunications spacecraft. The instrument began its normal operation in April 1997 and ended its mission in July 2002. The goal of this work was to use GORID's particle data to identify and separate the space debris to interplanetary dust particles (IDPs) in GEO, to more finely determine the instrument's measurement characteristics and to derive impact fluxes. While the physical characteristics of the GORID impacts alone are insufficient for a reliable distinction between debris and interplanetary dust, the temporal behavior of the impacts are strong enough indicators to separate the populations based on clustering. Non-cluster events are predominantly interplanetary, while cluster events are debris. The GORID mean flux distributions (at mass thresholds which are impact speed dependent) for IDPs, corrected for dead time, are 1.35×10^{-4} m^{-2}s^{-1} using a mean detection rate: 0.54 d^{-1}, and for space debris are 6.1×10^{-4} m^{-2}s^{-1} using a mean detection rate: 2.5 d^{-1}. β-meteoroids were not detected. Clusters could be a closely-packed debris cloud or a particle breaking up due to electrostatic fragmentation after high charging.

1. INTRODUCTION

A population of cosmic dust mixed with a population of man-made debris exists within the Earth's magnetosphere. Measurements of these provide the data samples for studies of the interplanetary dust particles that travel through our magnetosphere from the outside and for studies of the local byproducts of our space endeavors. Even though instruments to detect natural meteoroids and space debris particles have been flown in Low Earth Orbits (LEO) and on interplanetary missions, very

little information on the particle environment for Earth orbits above about 600 km altitude have been obtained. In particular, knowledge about debris particles smaller than 0.5 - 1 m in the geostationary (GEO) region was largely unknown before GORID.

2. REVIEW OF THE GORID DETECTOR AND ITS DATA

The GORID impact detector is the refurbished engineering model of the Ulysses dust detector, which detects particles by impact ionization methods (1; 2). In this method of detection, a particle impacting the detector at hypervelocity speed creates a plasma of electrons and ions. The electrons and ions generated during the impact are measured separately; the electrons are collected at the target (Qe), and the ions are collected at the ion collector (Qi). A few ions are further intensified and measured by a channeltron (Qc) behind the main ion collector grid. The negative (electron) and positive (ion) charges generated upon impact range from 10^{-16} C to 10^{-8} C. The charge on the particle itself, as it enters the detector, can be measured by the charge grids Qp.

The velocity and mass of the impacting particle are deduced from the rise-time and total intensity of the measured plasma signals using empirical calibration curves. The rise-times of the measured plasma signals are independent of the particle mass, and decrease with increasing particle speed. Given the sensitivity and the calibration of the instrument, GORID can detect particles with a mass down to 10^{-17} kg.

The instrument is a shallow cylinder with an entrance aperture of 43 cm and hemispherical target of area 0.1 m^2 and a viewing angle of 140°. The GORID detector was in a geostationary location at 80° East longitude until June 2000, when the satellite was moved to 103° East. Detailed information on the instrument design and data

handling is given in (3), and a full description of the instrument calibration and events classification is given in (4).

In the absence of any anomalies, the procedure to determine speeds and masses from GORID data is potentially straightforward: Laboratory calibration is applied to convert digital signals to: electron, ion and channeltron charges (Qe,Qi,Qc) particle speeds derived from target and ion collector rise-times (ve, vi). Debris particles are discriminated (statistically) by impact speed and timing of events (time of day, year, clustering). Constraints on individual derived orbits (based on speed and instrument pointing direction) can also be used. In general, determining the mass is via

$$Q = km^{\alpha}v^{\beta}, \qquad (1)$$

where k, α, and β are derived from laboratory calibration.

Extensive calibrations were performed for the twins of GORID: the Ulysses and Galileo dust detectors. Additional calibration tests for GORID confirmed that the established calibration was still applicable. The GORID signal amplitude calibration converts from digitized values of the signal amplitudes to amplitudes of charge Qe, Qi, Qc and Qp for the GORID dust detector. The calibration of the relationship between the speed of the impactor and the rise-time of the signals from the target and ion grid was performed using the Heidelberg Electrostatic Accelerator. The mass of an impacting particle can be derived from the charge to mass ratio for the ion or electron charge, as a function of velocity with a linear (power law) relationship: $\log(Q_i/m) = -1.063 + 3.375 \log(v)$ using calibration data supplied by E. Grün (MPI-K Heidelberg). The velocity calibration for the GORID dust detector converts from digitized values of rise-times for the target and ion grid signals to impactor impact speed (ve , vi).

Reliable impact speeds are the most important discriminator between interplanetary dust and debris. Accurate speeds are required for mass determination from impact charges because of the strong dependence on speed of the charge to mass ratio (Eqn. 1). Unfortunately, there is almost no correlation between the individual impact speeds derived from the ion and electron rise-times. The reasons for this poor correlation are not known, but could be due to a combination of the following: 1) noise can cause apparent slow rise-times, 2) high particle charges can also produce longer rise-times, 3) impacts on the sidewall of the detector (5). If we apply a single speed to all particles (e.g. a typical weighted mean interplanetary dust impact speed for GEO of 30 km s^{-1} it can introduce a potential error of up to 10^5 in mass for debris particles that in reality may have impact speeds as low as 1 km s^{-1}. This is due to the high value (3.4) of the velocity exponent β in Eqn. 1 from which the masses are derived.

Therefore the typical procedure to determine the impactor particle speeds, and hence, masses, could not be implemented. If we could find other characteristics of the

measurements for separating debris from the interplanetary (IP) dust, then mean speeds can be assigned and hence fluxes. One characteristic of the measurements is the charge.

3. DISTRIBUTION OF QP CHARGES

The GORID data contains many particles with apparent high charge. Table 1 illustrates the distribution of particle grid charges, Qp, for the highest quality GORID events. We divide the GORIDs charge grid detections (Qp) into five Qp classes (labelled A to E) which demonstrate peculiar charge values (high, negative) on the dust/debris particles.

Table 1. Distribution of Qp charges

Group	Qp	Number	Implied Properties
A	4×10^{-10}	463	Saturated
B	4×10^{-10}–10^{-12}	1191	High -v_e charge
C	10^{-12}–10^{-13}	1223	Medium -v_e charge
D	10^{-13}–0	205	Medium -v_e charge
E	> 0	230	+v_e charge

Since potentials are not expected to exceed 10 V (6), then we have either very large grains, (10 μm–10 cm), or the grain charging mechanism is not fully understood, or the Qp values are unreliable. We explored the Qp values further by checking the correlation for between electron and ion signals for -ve and +ve charges. The Qp data appear noisy with no systematic biases, therefore, we decided to use Qp as diagnostic property of charging. The individual Qp values may have large uncertainties, but it is possible that the charges can provide diagnostic information for distinguishing IP and debris populations, especially if coupled with another property of the impacts, temporal variations. In Sect. 5, we identify mechanisms that could produce high negative equilibrium potentials on short timescales. Next we describe the temporal variations of GORID's impacts.

4. TEMPORAL VARIATIONS

Temporal variations (clustering, diurnal, seasonal) may provide additional constraints for statistical separation of populations.

4.1. Clustering

Very large variations in daily event rates led to the identification of clusters of events, some of which re-occurred on consecutive days at the same local time (1; 7). They were interpreted as clouds of aluminium oxide debris resulting from the firing of solid rocket motors. IP dust particles, including β-meteoroids, have distributions in

space which are much larger than the scale of the GORID detector. Their arrival times are therefore expected to have a random distribution with a mean dictated by the particle flux for the particular pointing geometry of the detector. Clustering of events could occur if an IP particle fragments very shortly before impact, an extremely low probability event. Clustering of events is therefore indicative of a debris source and may provide a selection criteria for statistical separation of the debris and IP populations.

An event is defined to be a cluster member if the time interval to the closest event is less than a "clustering limit". The mean rate for the highest-quality impact events is 1.83 day^{-1}, corresponding to an interval of 0.55 d. The distribution of times between events (see Fig. 1) shows a bimodal distribution with one component peaking at about the expected "random" rate and the other with very much shorter times, indicating clustering. The limit of cluster membership is therefore defined at 0.05 days. IP particles would be expected to show approximately random time intervals (with a slightly wider than Gaussian spread due to the expected diurnal asymmetry). Typical time intervals between non-cluster events are $0.2 - 2$ days and for cluster events, seconds to ~ 1 hour. 74% of events are in clusters.
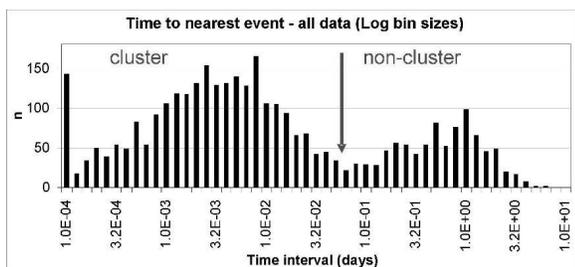

Figure 1. Distribution of time intervals between particle detections used to determine cluster and no-cluster membership.

The bimodal distribution of time intervals between events is apparent for all negative charge Qp classes. Qp class E data (positively charged particles) have no component of clustered events. Both the charge sign and the random nature of the detection times are consistent with Qp, class E events being entirely interplanetary in origin.

4.2. Diurnal and Seasonal Variation

Cluster events (Fig. 2) show very strong daily asymmetry whereas non-cluster data show a factor ~ 2.5 asymmetry with the peak around midnight local time, entirely consistent with an IP origin. Debris are concentrated near midnight local time except during summer. In early summer, clustered events are concentrated near 5 am, just at the time when β-meteoroids may be expected to be detected. However, there is no evidence for an enhancement in the non-clustered data at this time suggesting an alternative explanation for these events.
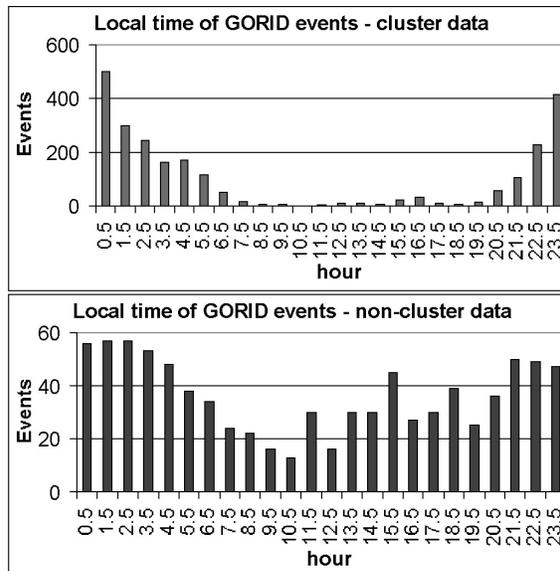
Figure 2. Distribution of impact detections as a function of time of day for cluster (upper panel) and non-cluster (lower panel) data.

4.3. Crossing of Equatorial Plane in Magnetotail

The GORID pointing geometry implies preferential detection of clusters, e.g. debris, after recent crossing of the equatorial plane in the magnetotail. This may be because debris are physically constrained to this region or because some process occurring in this region makes them detectable.

5. ON THE HIGHLY-CHARGED PARTICLES

Several competing mechanisms at 1 AU charge a debris or IP dust particle: photoelectric effect, electron and ion collection, and secondary electron emission. IP particles are expected to be positively charged (appearing in the Qp channel, E class). The situation for orbital debris is more complex. Field emission prevents further charging of a dust particle once it possesses a sufficiently strong surface potential.

If one assumes we have extremely highly-charged particles, then we can look at the dust charging conditions in GEO which might cause such an effect. Previous work (5) studied in depth the charging of dust/debris particles in Earth orbit from 2 R_E to 15 R_E (R_E = Earth radius = 6.378×10^6 m). It considered two ranges of magnetospheric activity: solar "typical" (or quiet) and solar "active" (or disturbed). The study used plasma data for typical earth plasma conditions, defined by $Kp=1$, $Ap=120$, and plasma data for active Earth plasma conditions, defined by $Kp=5$, $Ap=1200$. The study found that the charging currents of dust/debris particles are poised in a delicate balance, so that changes in the plasma parameters,

for example between quiet and disturbed plasma conditions, and changes in particle material properties can have large effects on the particles' charges. The next four cases (A,B,C,D) illustrate the variations of these charging effects. More details can be found in (5).

The next example illustrates conditions between quiet and disturbed plasmas when the material properties, as indicated in the next box, for charging the particle, remain the same. The equilibrium potential charges were calculated assuming currents for ion and electron collection from the plasma, photoelectric emission and secondary electron emission in a plasma with number densities and energies given in Table 2.

δ_{m}=1.4, E_{m}=180eV, χ=0.1, a=1μm, ρ=2.3g/cm^3, T_{photo}=2.0eV

Here, the particle material properties: δ_{m}, E_{m}, χ, a, ρ, and T_{photo} are the number of secondary electrons (yield) at a characteristic (maximum) energy at which the release of secondary electron peaks, the photoelectric constant (1 = fully conducting, 0.1 = fully dielectric), the radius and density of the particle, and the energy of the spectrum of the released photoelectrons in a Maxwellian distribution, respectively. Table 2 gives the changing plasma parameters, first, Case A, for a quiet plasma at 0 local time (Earth's shadow) in GEO, and second, Case B, for disturbed plasma at 0 local time in GEO.

Table 2. Plasma Parameters for Cases A & B

Plasma Type	n_{e} (1) (cm^{-3})	n_{i} (2) (cm^{-3})	kT_{e} (3) (eV)	kT_{i} (4) (eV)
Quiet	1.0 / 0.3	0.6 / 0.8	450 / 4000	12 / 9000
Disturbed	2.0 / 4.0	2.0 / 2.3	170 / 2400	40 / 11000

(1) Number densities for (hot/cold) electrons, (2) for (hot/cold) ions.
(3) Energies for (hot/cold) electrons, (4) for (hot/cold) ions.

The resulting equilibrium potentials are U_{pot}=2.2V (Case A) and U_{pot} =-2136.2V (Case B). The top charging process is the electron collection current. The latter equipotential current is high enough to be in the field emission range (5). One plausible reason for the high (theoretical) charge is multiple roots for equilibrium potential (8), which are especially important in plasmas with high temperatures or densities. For example, our numerical experiments that increased only the electron density in the plasma pushed the equilibrium potential to the next root, resulting in large negative potentials, when we increased the electron number density two and a half times (5).

The charging of the debris/dust particles is particularly sensitive to the secondary electron emission currents, so that a particle with surface properties of a low yield material can change from having an equilibrium potential a

few Volts positive to an extremely highly negative potential, assuming energetic or highly dense plasma conditions which did not change, as illustrated in the next two cases: C and D and Table 3. The material properties for the charging calculation are indicated in the boxes. Notice that the only changes between the two cases are the secondary electron yield (from 2.4 to 1.4) and the maximum energy for that secondary electron yield (from 400 to 180 eV).

δ_{m}=2.4, E_{m}=400eV, χ=0.1, a=1μm, ρ=2.3g/cm^3, T_{photo}=2.0eV, U_{pot}=3.7V *Case C*

δ_{m}=1.4, E_{m}=180eV, χ=0.1, a=1μm, ρ=2.3g/cm^3, T_{photo}=2.0eV, U_{pot}=-3034V *Case D*

Table 3. Plasma Parameters for Cases C & D

n_{e} (1) (cm^{-3})	n_{i} (2) (cm^{-3})	kT_{e} (3) (eV)	kT_{i} (4) (eV)
2.0 / 1.0	2.0 / 1.0	300 / 7000	300 / 7000

(1) Number densities for (hot/cold) electrons, (2) for (hot/cold) ions.
(3) Energies for (hot/cold) electrons, (4) for (hot/cold) ions.

6. DERIVED FLUXES AND MASS DISTRIBUTIONS

In the absence of any reliable speed determination, mean speeds are assigned for debris (clustered) and IP (non-clustered) events. Fluxes are then determined by multiplying the speeds with the number of particles in a unit time and integrating over the GORID detecting surface.

Representative impact speeds for IP particles and space debris are assigned for non-clustered and clustered events respectively. For IP particles, we used an IP model (9), which gives a speed distribution weighted by the impact plasma detector response $v^{3.4}$, with which we find a mean speed of 31.4 km s^{-1}. For debris particles, we used the following. Particles in near-GEO orbits will have impact speeds of a few hundred meters per second. However, at these low speeds, they are not likely to produce large amounts of impact plasma. The dominant contribution (i.e. highest relative speeds) of debris are expected from impactors in geo-transfer orbits (GTO). The weighted (by response/geometry/source) mean speed = 2.6 km s^{-1}. For accessible retrograde GTO orbits, v = 4.5 km s$^{-1,}$ and for circular retrograde GEO orbits v_{max} = 6.1 km s^{-1}.

The GORID raw data files gave the number of particles per unit time. The data from the GORID experiment is distributed in three different sets of files: science, count, and housekeeping files. Details of the data format can be found in: (10). The total number of the highest quality events in the science file is 3349 (2477 clustered, 872

non-clustered) in 1827 days. In the count file data there are ∼5486 events. We can use the known properties of the science data to assign the count file events as either IP or debris before calculating the fluxes.

After the counts are determined from the data files, they were corrected for "dead time". Interplanetary events, which are detected essentially at random, suffer a "dead time", equivalent to the clustering time of 0.05 days. The total dead time for IP (i.e. non-clustered) detections is 0.05 × 3349 = 167 d, so that the dead time correction is = 1827/(1827-167) = 1.101. Therefore, the total expected number of interplanetary events is 872 × 1.101 = 960. The detection rate of interplanetary events from the science data file is 960/1827 = 0.53 d^{-1}. The dead-time interval is slightly higher due to events in the count files, which exceed the maximum event number of the count buffer of the instrument. After correcting for the 28 additional events, the total number of IP events is 988. The total detection time is 1827 d giving a mean interplanetary flux of 0.54 d^{-1}.

The space debris flux is therefore calculated from all remaining events detected, i.e. 5486 − 988 = 4498 in 182 d. The mean debris detection rate is therefore 2.46 d^{-1}.

Cumulative fluxes are calculated for an equivalent flat plate detector pointing in the same direction as GORID, which has a detector area A = 0.1 m^2 and effective viewing angle of Ω = 1.45 sr: $F(\succ Q_i)$ = $(N(\succ Q_i) \; f \; (\pi/\Omega)) \; / \; (T \; A)$, where $N(\succ Q_i)$ is the number of events with ion grid charge greater than Q_i, f is a scaling factor to account for missing data (due to dead time and count file data, and T is the time interval over which the observations were made. Figure 3 shows the calculated cumulative fluxes for cluster and non-cluster data. The ion grid signals are saturated at $Q_i = 2 \times 10^{-10}$ C. The debris (cluster) data show relatively greater fluxes at smaller charges.
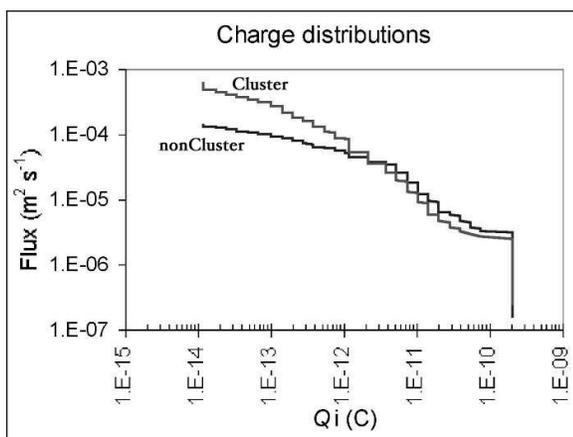

Figure 3. Cumulative fluxes on GORID as a function of ion grid charge.

Figure 4 shows the cumulative mass distributions derived using representative single values of impact speed for debris (cluster) and IP (non-cluster) events compared with the interplanetary model described in (9). The calculated interplanetary flux in GEO is lower than the model by a factor of between 2 and 10 even though this model provides a good fit to impact cratering data measured on spacecraft in LEO. The assumption of a single velocity is important. The distribution of speeds of interplanetary dust ranges from a few to 70 km s^{-1} and the speed distribution used in the model, derived from meteor data, may not precisely apply to the smaller particles detected by GORID. A factor of 2 error in speed results in a factor of 10 error in mass because of the v$^{3.4}$ power relationship between impact speed and derived mass for a given impact charge (Eqn. 1). The flux is defined by the measured impact rate. A higher impact speed would result in lower masses for the entire distribution and hence a lower flux at any specific mass (the actual error in flux would depend on the mass distribution but would also be a factor of 10 for a mass distribution index of -1). In addition, the data have been converted from GORID detections to fluxes seen on a flat plate detector pointing in the same direction. Debris fluxes are calculated for the nominal mean impact speed for GTO of 2.6 km s^{-1} and for the maximum possible GTO impact speed of 4.5 km s^{-1}. In both cases, much higher fluxes are observed for debris than interplanetary particles in this size range. Debris fluxes appear to be ∼20 times the interplanetary flux model for masses below 10^{-14} kg.
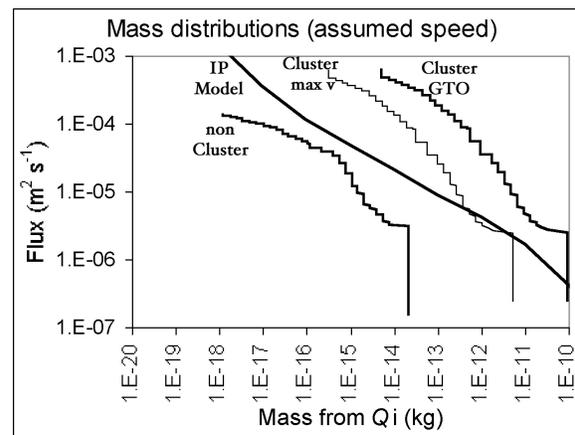

Figure 4. Cumulative mass distributions derived using a mean impact speeds for interplanetary dust of 31 km s^{-1} applied to non-cluster data and either a mean (2.6 km s^{-1}) or maximum (4.5 km s^{-1}) GTO impact speed for cluster data. An interplanetary dust model prediction (9) is shown for comparison.

We can test if the fluxes derived using the impact speeds of GTO particles are reasonable by estimating the total mass of dust in the GTO population. If we make a simple assumption of uniform spatial density of debris in a spherical cloud from altitudes of 1000 km to GEO and a particle mass of 10^{-14} kg, we derive a total mass of such particles around the Earth of a few hundred kg. This is likely to be an overestimate because particles spend a large fraction of their orbital time near apogee and the orbital distribution of the presumed sources have non-uniform inclination distributions and apsides close to the

equatorial plane. Alternatively, some of the debris particles may be moving significantly faster than the assumed speed, and hence be much smaller, their large charge causing acceleration in the magnetosphere. Without reliable impact speeds it is not possible to determine the true fluxes to high precision. Uncertainties in mass of a least a factor of 10 are inevitable.

7. SUMMARY AND FUTURE WORK

Although the speeds derived from rise-times in GORID data are not reliable, the clustering of events can be used to discriminate between space debris and interplanetary particles. The detection rate of interplanetary events is 0.54 d^{-1} and debris events is 2.46 d^{-1}. The mean fluxes are 1.35×10^{-4} m^{-2} s^{-1} for IP and 6.1×10^{-4} m^{-2} s^{-1} for debris at the detection threshold of $Q_i = 1.3 \times 10^{-13}$ C. The fluxes of interplanetary particles are reasonably close to the well-defined model prediction, allowing for the impact speed uncertainty. Detectability of debris may be influenced by charging mechanisms in the magnetosphere.

One possible explanation for the clusters could be a closely-packed debris cloud or a slag particle breaking up under electrostatic fragmentation. Work by (11) demonstrated that a debris cloud from a GEO insertion burn could stay together for weeks and months to give multiple impacts with the same time stamp. A different work by Felix van der Sommen (personal communication) showed that a closely-packed debris cloud originating near GEO could be detected by GORID as a cluster, if: 1) initial velocities are very low, and 2) they are charged enough. Another possibility is electrostatic fragmentation, which has been considered for clustered phenomena in the Earth's magnetosphere before (e.g. (12)). Slag particles from a rocket GTO or GEO burn might fragment upon entering the highly energetic environment of the magnetospheric plasma sheet. These possibilities need to be investigated further.

REFERENCES

[1] Drolshagen, G., Svedhem, H., Grün, E., Grafodatsky, O., and Prokopiev, U. Microparticles in the geostationary orbit GORID experiment. *COSPAR*, 1998.

[2] Drolshagen, G., Svedhem, H., and Grün, E. Measurements of cosmic dust and micro-debris with the GORID impact detector in GEO. *Proc. Third European Conference on Space Debris ESOC*, ESA SP-473, 2001.

[3] Grün, E., Fechtig, H., Giese, R. H., Kissel, J., Linkert, D., Maas, D., and McDonnell, J. The Ulysses dust experiment. *Astron. Astrophys. Suppl. Ser.*, 92:411–423, 1992.

[4] Grün, E., Baguhl, M., Hamilton, D., Kissel, J., Linkert, D., Linkert, G., and Riemann, R. Reduction of Galileo and Ulysses dust data. Technical report, Max-Planck-Institut für Kernphysik, 1994.

[5] McDonnell, J. Update of statistical meteoroid/debris models for GEO, final report of ESA contract 13145/98/nl/wk. Technical report, European Space Agency, July 2000.

[6] Mukai, T., Blum, J., Nakamura, A. M., Johnson, R., and Havnes, O. *Interplanetary Dust*, chapter Physical processes on interplanetary dust, pages 445–507. Springer Verlag, Heidelberg, Germany, 2001.

[7] Svedhem, H., Drolshagen, G., Grün, E., Grafodatsky, O., and Prokopiev, U. New results from in-situ measurements of cosmic dust data from the GORID experiment. *Adv. Space Res.*, 289:309–314, 2000.

[8] Meyer-Vernet, M. 'Flip-flop' of electric potential of dust grains in space. *Astr. Ap.*, 105:98–106, 1982.

[9] McBride, N. and Hamilton, D. Meteoroids at high altitudes, final report of ESA contract 13145/98/nl/wk. Technical report, European Space Agency, July 2000.

[10] McDonnell, J. Processing, analysis and interpretation of data from impact detectors, final report of ESA contract 16272/02/nl/ec. Technical report, European Space Agency, July 2004.

[11] Bunte, K. The detectability of debris particle clouds, for final report of ESA contract 16272/02/nl/ec. Technical report, European Space Agency, July 2004.

[12] Fechtig, H., Grün, E., and Morfill, G. Micrometeoroids within ten earth radii. *Planetary and Space Science*, 27:511–531, April 1979.